Time-domain acoustic pressure fields from axisymmetric impulse sources by Rayleigh's Integral

Stephen Warshaw

40 West 15th St Loft 1C, New York, NY 10011, USA
siw1939@yahoo.com

This paper shows how Rayleigh's Integral can be used to efficiently and rapidly calculate time-domain pressure waveforms and wavefronts radiated from a planar baffle due to axisymmetric normal impulse accelerations that converge toward or expand away from a fixed center of symmetry. These accelerations are prescribed with simple functional forms and histories. The Rayleigh Integrals are evaluated by Gaussian quadratures that seem peculiarly suited to the integrands. The acoustic fields are presented as "snapshots" of pressure contours of the evolving wavefront structures emerging from the baffle surface, and as functions of time at given points. Significant insights are provided by graphs of slant range versus time that identify signal paths from the source points to the field points. The presented methods avoid the complexities inherent in more standard transform and harmonic source treatments.

1 Introduction

In his original derivation of the integral expression that bears his name, Rayleigh [1] employed solutions of the linear wave equation to formulate an integral describing small amplitude air pressure waves emitted by vibrations of a finite surface area in an infinite planar baffle. In modern notation, the time-domain form of this integral can be written [2]

$$p = \frac{\rho_0}{2\pi} \int a_n(t - R/a_0) \frac{d\sigma}{R}$$

where p is the acoustic pressure function at some field point off a planar baffle, $d\sigma$ is the element of active area in the baffle surface, a_n is the normal component of surface acceleration at the retarded time $t - R/a_0$ (and the source of the sound pressure), R is the distance between the field point and the surface element, and a_0 and ρ_0 are the speed of sound and density, respectively, of the ambient air, assumed uniform.

Many theoretical developments and ideas about transient radiation from baffled surfaces have followed from this first exposition [3 – 10], but experimental work to verify that the Rayleigh integral can accurately account for acoustic pressure fields emitted by pulsed surfaces in the time domain is sparse. Banister and Hereford [11] have reported on measurements of acoustic pulses at high altitudes above a ground surface impulsively moved upward by a buried underground explosion. They carried out Rayleigh integral calculations using measured vertical motions of the ground as source functions, and accounted for the observed pulse measurements with moderate success. Two large and sharp vertical acceleration spikes that appear in most of their data suggest that the Rayleigh integral could predict real-world pulsed waveforms when Dirac delta functions are actually used as the source motion acceleration.

In this proceedings paper, we investigate this concept and present mathematical details and graphical results of the use of Rayleigh's integral to compute acoustic fields generated by a delta function ring uniformly expanding away from a center of symmetry [12]. We also present wavefront and waveshape calculations for other types of impulse source configurations in the poster session of the conference. Our results suggest the intriguing possibility that the time-domain Rayleigh integral for delta function type sources can be valid even at field points very close to the source plane. The author feels that experimental investigation of this possibility would be an extremely worth while effort, and easily realized with current transducer technology.

2 Mathematical Formulation

We consider the Rayleigh integral for a planar impulse function source such that its normal acceleration is a "delta function ring" distribution having the general axisymmetric form $a_n = f(r)\delta(t - g(r))$, where f and g are functions of the radial distance r from a fixed center of symmetry in the plane. (Asymmetrically distributed motions are not treated here; others have reported Rayleigh integral developments for such cases, see, e.g. [6, 7, 9 ,10].) We then specialize to the case where the ring radius r expands at a uniform radial velocity v_s, that is, $a_n = \delta(t - r/v_s)$, and the motion stops at a finite radius $r = a$. (When v_s becomes infinite, we recover the well-known case of the impulsively accelerated disk.)

The geometry and coordinate system used here is shown in Figure 1, where the rigid baffle lies in the x–y plane, the source motion center lies on the y-axis at a distance b from the origin, and the field observation point is on the z-axis at a distance c above the baffle plane. The source motions lie within a disk of radius a. We represent the expanding impulsive ring by a circle of changing radius r in the x–y plane. The area element $d\sigma$ is shown as a small oblong on this circle. The distance from $d\sigma$ to the field point is represented by R, and that from the origin to $d\sigma$ by a line of length ρ that makes an angle ϕ with the y-axis.

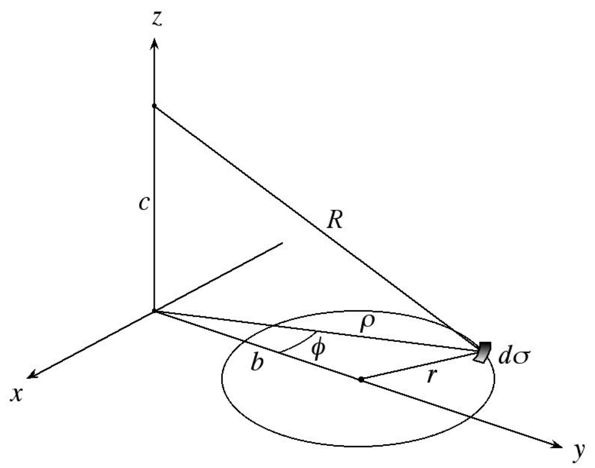

Figure 1. Geometry for the impulsive Rayleigh integrals presented in this paper. The observation point is c units above the x–y plane and b units horizontally displaced from the source center of symmetry.

The relations $R^2 = \rho^2 + c^2$ and $r^2 = \rho^2 + b^2 - 2\rho b \cos\phi$ clearly hold. From them we obtain

$$d\sigma \;=\; \rho\, d\phi\, d\rho \;=\; 2\, r\, R\, dr\, dR \Big/ \sqrt{Q(r,R)}$$

where

$$Q(r,R) \;=\; (2b\rho)^2 \;+\; (\rho^2 \;+\; b^2 - r^2)^2.$$

Then the integral becomes

$$I \;=\; \frac{2\pi p}{\rho_0} \;=\; 4\int_c^{\infty}\int_0^{a} \frac{r\, f(r)\; \delta(t - g(r) - R/a_0)}{\sqrt{Q(r,R)}}\; dr\; dR$$

We integrate over the variable r first, with the result

$$I \;=\; \frac{2\pi p}{\rho_0} \;=\; 4\int_c^{\infty} \frac{r_0\, f(r_0)\,\left[H(a - r_0) \;-\; H(-r_0)\right]}{|g'(r_0)|\sqrt{Q(r_0,R)}}\; dR$$

where r_0 is the zero of the delta function argument, and solves the equation $g(r) = t - R/a_0$. $g'(r_0)$ is the slope of the delta function argument at this zero crossing, and behaves as a scale factor. (One recalls that the integral of $\delta(kx)dx$ is $1/k$.) The H functions are Heaviside unit step functions, where $H(x)$ is 1 for $x > 0$ and zero for $x < 0$, and arise from integrating a delta function over a finite interval. a is the limit of r at which the source motion ends.

Certain properties of this integral can immediately be deduced, and are also presumed to hold for any $f(r)$ and $g(r)$. First, if the delta function argument has more than one zero, then a separate integral exists for each zero, and each such integral contributes to the overall response I at the field point. Second, and by definition, r_0 is necessarily a function of R and t, and thus gives I its time-varying character. Third, for fixed value of t, the above integral can be evaluated to give the value of I at that time t. In this evaluation, the Heaviside function difference defines the range in R over which the integrand does not vanish, and therefore augments the integration limits. In a similar consideration, physically meaningful parts of the integral exist only for those values of R that give the function Q in the radical a positive value, and so the zeros of Q augment the integration limits as well. Thus, we have the crucial circumstance that *each such limit of integration is also a function of time*. This aspect will become quite apparent in all the examples we discuss.

3 Expanding Impulse Ring

We consider an impulsive ring of constant amplitude which uniformly expands from a given point with radial velocity v_s and stops when it reaches a radius $r = a$. Then $f(r) = 1$ and $g(r) = r/v_s$, and the delta function argument is zero when $r/v_s = t - R/a_0$. Thus, the zero of the argument is $r_0 = v_s t - \beta R$. For notational convenience, we have defined a "source Mach number" as $\beta = v_s / a_0$, which is the ratio of the source ring expansion constant velocity to the speed of sound in the air.

The integration interval is defined partly by the Heaviside function difference in the integrand, and partly by the requirement that the radical in the integrand be real. For this expanding ring case, the function in the radical is

$$Q(r_0,R) \;=\; 4b^2\left(R^2 - c^2\right) - \left(R^2 - c^2 + b^2 - \left(v_s t - \beta R\right)^2\right)^2.$$

This expression factors conveniently into a product of four linear terms, that is,

$$Q(r_0,R) \;=\; -(\beta^2 - 1)\prod (R - R_i)$$

where the four roots R_i are given by

$$\left(\beta^2 - 1\right)R_i \;=\; \beta\left(v_s t \;\pm\; b\right) \;\pm\; \sqrt{\left(\left(v_s t \;\pm\; b\right)^2 - \left(\beta^2 - 1\right)c^2\right)}$$

and where each root has a different pairing of the + and − signs applied to the radical and the constant b. Then

$$I \;=\; \frac{4a_0\beta^2}{\left|\beta^2 - 1\right|}\int_c^{\infty} \frac{(a_0 t - R)\; dR}{\sqrt{-\,(R - R_1)(R - R_2)(R - R_3)(R - R_4)}}$$

It is clear that for any given field point location (i.e., for fixed b and c), each root R_i is a function of t, and a plot of slant range R versus time t showing all four roots proves to be highly instructive and useful. A representative such plot is shown in Figure 2 for fixed values of a, b, and c, for a supersonic source where $\beta > 1$.

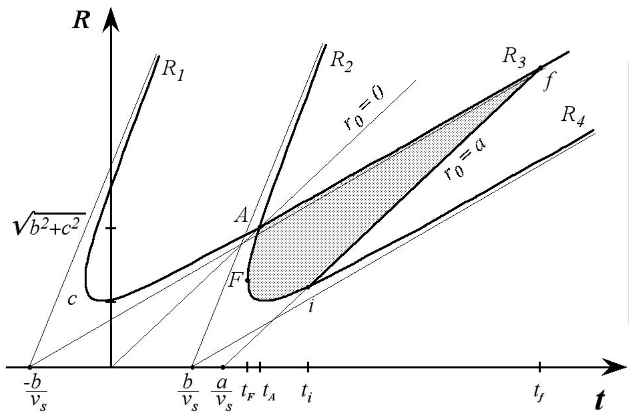

Figure 2. Root loci hyperbolas, their asymptotes, and Heaviside argument zero straight lines plotted as distance R of source point to field point versus time t, for a given fixed value of a, b and c. The labeled features are explained in the text.

We chose $a > b$, so that the observation point lies directly above part of the source region $r < a$. The root loci $R_i(t)$ form upper branches of two intersecting hyperbolas in the $R - t$ plane. These are given by the following two equations (one for each value of the sign of b):

$$\left[(\beta + 1)R - \left(v_s t \pm b\right)\right]\left[(\beta - 1)R - \left(v_s t \pm b\right)\right] + c^2 = 0$$

The zeros of the Heaviside functions (at $r_0 = 0$ and $r_0 = a$) are also functions of time, and each plots as the straight lines shown in the Figure.

The shaded region in the figure (bounded by the Heaviside zero lines and the quartic root loci) defines the domain of R and t in which the Rayleigh integral integrand is real and exists. The maximum and minimum values of R at each t in this domain thus provide the required integration limits for the evaluation.

The boundary of this shaded region also contains information explaining some features of the resulting pulse. The pulse starts at time $t_F = (b + c\sqrt{(\beta^2 - 1)})/v_s$ corresponding to the Fermat path of minimum travel time for any acoustic information to reach the field point; and the corresponding slant distance is $R_F = \beta c\sqrt{(\beta^2 - 1)}$. The onset of source motion (t = 0) reaches the field point at $t_A = R_A / a_0$ where the slant distance is $R_A = \sqrt{(b^2+c^2)}/a_0$. The points and time marks labeled by i and f identify signals reaching the field point from the near and far edges of the motion limit circle $r_0 = a$; and the corresponding slant distances and times are $R_{i,f} = \sqrt{(c^2 + (b \pm a)^2)}$ and $t_{i,f} = a/v_s + R_{i,f} / a_0$. For this configuration (where $b < a$) the time of the minimum of R at c is $t_C = b/v_s + c/a_0$.

To round out this discussion, we observe that for any point within the source region $r < a$, the time of signal reception from that point is $t = r/v_s + R/a_0$, while the extremes in slant range R for this circle are $R^2 = c^2 + (b \pm r)^2$. On combining these two expressions by eliminating r, we recover the condition $Q(r_0,R) = 0$. We thus see that two of the four roots of this quartic equation correspond to these extremum paths during the source time interval.

4 Integration Methods and Pulse Synthesis

The Rayleigh integral for the expanding ring is clearly an elliptic integral. We have chosen to evaluate it by efficient Gaussian quadrature techniques which seem appropriate to this task. For the specific situation represented by Figure 2 three distinct integration ranges are evident, corresponding to the time intervals t_F to t_A, t_A to t_i, and t_i to t_f.

In the first time interval [t_F, t_A], the integration range is R_4 to R_2 and each limit is a root (i.e., a zero) of the integrand denominator. Gauss-Chebychev quadrature [13] appears to be well-suited for calculating the Rayleigh integral between these singularity limits when the integrand is recast in the form $h(R)/\sqrt{(-(R - R_4)(R - R_2))}$. Then the integral is evaluated by the following sum over N points:

$$I = \frac{\pi}{N}\sum_{k=1}^{N} h(\xi_k) \text{ where } 2\xi_k = (R_2 + R_4) + (R_2 - R_4)\cos\left(\frac{2k-1}{2N}\pi\right)$$

In the second time interval [t_A, t_i], the integration range is R_4 to R_3, and Gauss-Chebychev quadrature also applies, with R_3 replacing R_2.

In the third time interval [t_i, t_f], the integration range is from R on the radial limit line $r_0 = a$ to the root R_3, and only at R_3 is the limit a singularity. The distance R at the limit line is $R_0 = (v_s t - a)/\beta$, and so the integration interval is R_0 to R_3. The integrand is then recast in the form $p(R)/\sqrt{(R_3 - R)}$, and modified Gauss-Legendre quadrature [14] easily evaluates it as the following sum over N points:

$$I = 2\sqrt{R_3 - R_0} \sum_{k=1}^{N} w_k p(\xi_k)$$

In this expression, w_k is the Gauss-Legendre weight factor, and $\xi_k = R_3 - (R_3 - R_0)\zeta_k^2$, where ζ_k is the k^{th} positive zero of the Legendre polynomial $P_{2N}(\zeta)$.

In all three cases, N = 8 provides ample accuracy, and the corresponding algorithms can be extremely efficient.

In Figure 3 we plot a representative pulse (as a function of time) corresponding to the root loci shown in figure 2 that results from carrying out the indicated quadratures for the indicated time intervals. The initial "Fermat jump" at t_F, and "edge falloff" profile between t_i and t_f are clearly evident. An interesting feature of this pulse is the apparent dip in the initial plateau at the time t_C corresponding to the minimum R at $R = c$. When β becomes infinite (thus modeling the well-known impulsively accelerated disc [3]) this "dented" plateau becomes flat.

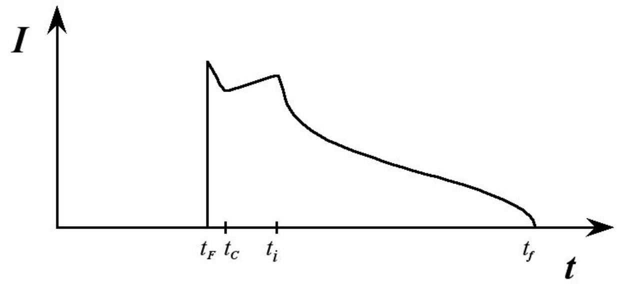

Figure 3. Representative pulsed waveform corresponding to the quartic root and Heaviside function argument arrangement shown in Figure 2.

5 Pulse "Snapshots"

We have used these integration evaluations at a sufficiently large number of pairs of values of b and c to calculate "snapshots" of the acoustic pulse field emerging upward from a supersonically expanding pulsed ring in a baffle plane. Figure 4 shows this as a sequence of plots of contours of acoustic pressure, starting with the first "snapshot" in the bottom plot.

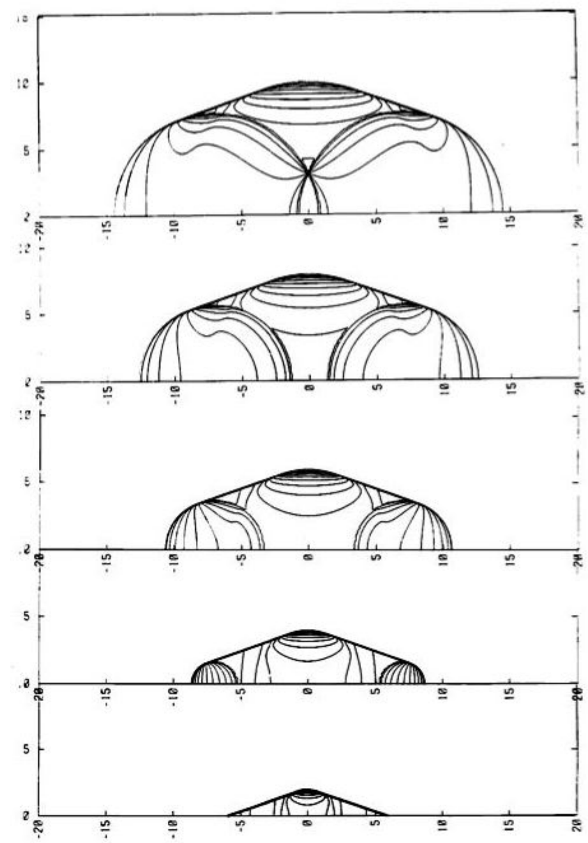

Figure 4. Two-dimensional plots of isobars in a pulsed waveform launched by a horizontally expanding supersonic ring source as viewed from the side, shown at equal time increments, starting at the bottom. Contour, horizontal (r) and vertical (z) scales are the same in each plot, but are otherwise arbitrary.

In these snapshot plots, the ring source expansion velocity is 3 times the speed of sound in air ($\beta = 3$), and the impulse source region in the $z = 0$ plane extends from $r = -7$ to $r = +7$. Thus, the source limit is $a = 7$. The first plot at the bottom shows the source expanded to $r = 6$. The time it took the source to reach this radius is also the time increment between the subsequent ascending pulse plots above it. The double semicircle feature (actually, the trace of a half torus in section) over the source stop points r = 7 and r = −7 that are apparent in the second and later snapshots, represents the acoustic "break" signal originally generated when the source stopped at its radial limit.

6 Conclusions and a Look Forward

We have shown, using simple algebraic manipulations, how a Rayleigh integral having an expanding delta function surface motion source can be used to predict realistically appearing wavefront and waveforms launched from the moving surface into the air into all regions, from right at the source surface to further on out. We also demonstrated how an expanding acceleration impulse moving supersonically across the source plane can produce -- as the contour plots in Figure 4 indicate -- a rising acoustic pancake "bow wave" caused by this motion.

We have found that numerically accurate evaluations of the Rayleigh integral are obtained rapidly and expeditiously with just 8-point Gaussian quadrature techniques; as the smoothness of the contour plots shown in Figure 4 attests. One may then contemplate fruitfully using such techniques in larger scale propagating pulse simulations from more complex delta function sources.

Carrying these notions toward future work, we observe that when a deeply buried explosive is detonated, a more-or-less spherically expanding underground blast wave produces an expanding, impulsive acceleration ring at the ground surface above it right after the blast wave arrives at this boundary. The author believes that a good part of the ascending aeroacoustic waveforms that were measured by Banister and Hereford [8] can be adequately accounted for by modeling these measured ground surface accelerations as delta functions with appropriate kinematic arguments.

In the accompanying poster session we will present preliminary kinematic calculations for a rising acoustic waveform caused by a surface delta function impulse ring that follows the surface trace of a spherically expanding underground blast wave. For this case the delta function argument contains g(r) = $\sqrt{(r^2 + z^2)}/v_s$ where v_s is now the speed of expansion of the blast wave, and z is the depth at which the explosion is located. The quartic root loci now have an aspect that is not as purely hyperbolic as are the ones shown in Figure 2. The techniques for calculating the rising acoustic field are otherwise almost identical to the procedures presented here.

Finally, our calculational procedures can be applied with almost no change to the case of a contracting ring source, that is, where the delta function ring in the planar baffle starts at $r = a$ and converges uniformly to $r = 0$. These developments will also be presented in the poster session.

References

[1] J. W. S. Rayleigh, *The Theory of Sound*, Vol. 2, 2nd ed. (1896). Dover, NY reprint (1945), section 278.

[2] A. D. Pierce, *Acoustics*, Acoustical Society of America, NY, 1989 edition, section 5-2

[3] *ibid.*, sections 5-6, 5-7 and footnotes

[4] P. R. Stepanishen, *J. Acoust. Soc. Am.* **49**, 1628 (1971)

[5] G. R. Harris, *J. Acoust. Soc. Am* **70**, 10 (1981)

[6] G. R. Harris, *J. Acoust. Soc. Am* **70**, 186 (1981)

[7] P. R. Stepanishen, *J. Acoust. Soc. Am.* **70**, 1176(1981)

[8] R. M. Simonds, *J. Acoust. Soc. Am* **78**, 244 (1985)

[9] J. F. Kelly and R. J. McGough, *J. Acoust. Soc. Am* **121**, 759 (2007) and references cited

[10] T. Mellow, *J. Acoust. Soc. Am* **123**,1880 (2008)

[11] J. R. Banister and W. V. Hereford, *J. Geophys. Res.* **96**(D3), 5185 (1991)

[12] S. I. Warshaw, *J. Acoust. Soc. Am*. **77**, S60 (1985); *J. Acoust. Soc. Am.* **79**, S90 (1986); *J. Acoust. Soc. Am.* **80**, S106 (1986); and *12 ICA Toronto*, Paper L3-6 (1986)

[13] M. Abramowitz and I. A. Stegun, *Handbook of Mathematical Functions*, Dover, NY 1972, p. 889, Formula 25.4.39

[14] *ibid.*, Formula 25.4.37